

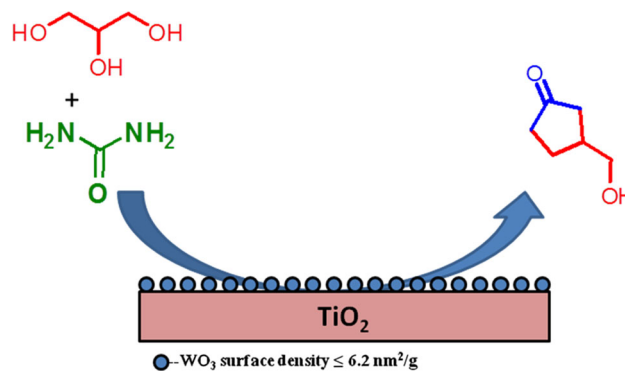
# The Role of Tungsten Oxide Species Supported on Titania Catalysts for the Synthesis of Glycerol Carbonate from Glycerol and Urea

K. Jagadeeswarai<sup>1</sup> · Ch. Ramesh Kumar<sup>1</sup> · A. Rajashekar<sup>1</sup> · A. Srivani<sup>1</sup> · N. Lingaiah<sup>1</sup>

Received: 6 January 2016 / Accepted: 8 January 2016 / Published online: 22 January 2016  
© Springer Science+Business Media New York 2016

**Abstract** A series of  $\text{WO}_3$  supported on  $\text{TiO}_2$  catalysts were prepared by impregnation method with varying  $\text{WO}_3$  content. The prepared catalysts were characterized by FT-IR, Laser Raman, X-ray diffraction, BET surface area and temperature programmed desorption of  $\text{NH}_3$ . X-ray diffraction and Laser Raman spectroscopic results suggest that  $\text{WO}_3$  was highly dispersed on titania up to 15 wt%. Acidity of the catalyst depended up on  $\text{WO}_3$  loading on titania and calcination temperature. The catalyst with 15 %  $\text{WO}_3$  content calcined at 500 °C exhibited high surface area and high acidity. Activity of the catalysts was evaluated for the synthesis of glycerol carbonate from glycerol and urea. The catalytic activity results showed that 15 %  $\text{WO}_3$  supported on  $\text{TiO}_2$  exhibited about 73 % glycerol conversion with near 100 % selectivity for glycerol carbonate. The influence of support on glycerol conversion was also studied and activities for different supports were in the order of  $\text{TiO}_2 > \text{SiO}_2 > \text{MoO}_3 > \text{Nb}_2\text{O}_5 > \text{ZrO}_2 > \text{Al}_2\text{O}_3$ . Different reaction parameters were also studied and optimum conditions were established. The catalyst is reusable without considerable loss in activity.

## Graphical Abstract



**Keywords** Glycerol · Glycerol carbonate · Titania · Tungsten oxide · Urea

## 1 Introduction

Glycerol, a by-product of biodiesel industry, is a potentially important biorefinery feedstock [1, 2]. Glycerol have a great number of common applications and have been used in pharmaceuticals, cosmetics, soaps, toothpastes, candies, cakes and as a wetting agent in tobacco [3, 4]. Even though it has lot of applications, it is creating a glut in the global market due to the increasing production of biodiesel [5]. The usage of low-grade glycerol obtained from biodiesel is a big challenge, as this glycerol cannot be used for food and cosmetic applications [3]. An effective usage or conversion of glycerol to specific products will cut down the biodiesel production costs [6]. Glycerol is a highly functionalized molecule and a variety of value

✉ N. Lingaiah  
nakkalingaiah@iict.res.in

<sup>1</sup> Catalysis Laboratory, Inorganic & Physical Chemistry Division, CSIR–Indian Institute of Chemical Technology, Hyderabad, Telangana 500 007, India

added chemicals can be produced by catalytic conversion through different reactions [7]. Catalytic conversion of glycerol to value added chemicals by green catalytic process is a challenging area of research.

Among the different possible products, glycerol carbonate is one of the important chemical which has excellent properties such as low toxicity, good biodegradability and high boiling point. Glycerol carbonate has application in gas separation membranes, polyurethane foams and surfactant component [8–10]. It is also used in coatings and paint industry [11]. There are several methods reported for the preparation of glycerol carbonate. It can be prepared by the reaction of glycerol with phosgene [12], glycerol transesterification with dialkyl carbonate or alkylene carbonate [13], carbonylation by urea [14]. Glycerol carbonate can be synthesized through the reaction of glycerol with carbon monoxide and oxygen in the presence of a catalyst [15]. Alternative routes such as transesterification reaction of glycerol with dialkyl or alkene carbonates to obtain cyclic carbonates have been explored [16–19]. The direct reaction of glycerol with CO<sub>2</sub> appears very attractive, but it has thermodynamic limitations [20]. Supercritical CO<sub>2</sub> was also attempted using zeolites as catalysts [21]. The foregoing observations led to consider urea as an alternative source for carbonylation of glycerol. The main advantage of this method is that to use urea which is readily available and cheap. The reaction is carried out in the absence of solvent and the only significant by-product is ammonia in the gas phase which can be easily captured. Various base catalysts have been tested for the synthesis of glycerol carbonate from glycerol and urea [13, 22–38]. Inorganic salts such as ZnSO<sub>4</sub> [22, 23] and MgSO<sub>4</sub> [24, 25] are effective homogeneous catalysts. Compared to these homogeneous ones, heterogeneous catalysts may be more useful for post-reaction procedures like easy recovery and reuse of catalysts. Several authors studied the performance of solid catalysts including La<sub>2</sub>O<sub>3</sub> [26], Au nanoparticles [27], Co<sub>3</sub>O<sub>4</sub>/ZnO [28], MgO, CaO and mixed metal oxides like Al/MgO<sub>x</sub>, Al/LiO<sub>x</sub> prepared from hydrotalcites [13],  $\gamma$ -zirconium phosphate [29], metal-exchanged heteropoly tungstate catalysts [30, 31], Sn–W mixed oxide catalysts [32], metal monoglycerolates [33], silicotungstate/MCM-41 [34], metal ion-exchanged zeolites [35], waste boiler ash [36], gypsum based catalyst [37], and organic–inorganic hybrids of imidazole complexes of zinc (II) [38] etc. Although some of useful catalysts are reported, still there is a need to develop highly active heterogeneous catalysts that works under mild reaction conditions.

In the present study, a series of WO<sub>3</sub> supported on TiO<sub>2</sub> catalysts with varying WO<sub>3</sub> content were prepared and studied for the synthesis of glycerol carbonate from glycerol and urea. The role of WO<sub>3</sub> on TiO<sub>2</sub> for the synthesis of glycerol carbonate is discussed with the observed physico-chemical properties of the catalysts.

## 2 Experimental

### 2.1 Catalyst Preparation

A series of catalysts with varying WO<sub>3</sub> content from 5 to 25 % supported on TiO<sub>2</sub> were prepared by impregnation method. The required quantity of ammonium metatungstate was dissolved in distilled water and this solution was added to the support with continuous stirring. The excess water was removed on water bath. The resulting solid was dried at 100 °C for overnight and finally calcined at 500 °C for 4 h. These catalysts were denoted as x % WO<sub>3</sub>/TiO<sub>2</sub>, where x indicates the weight percentage of WO<sub>3</sub> on titania.

### 2.2 Characterization of the Catalysts

X-ray powder diffraction patterns were recorded on a Rigaku Miniflex diffractometer using Cu K $\alpha$  radiation (1.5406 Å) at 40 kV and 30 mA and secondary graphite monochromatic. The measurements were obtained in steps of 0.045° with count times of 0.5 S, in the 2 $\theta$  range of 5–80°.

Confocal micro-Raman spectra were recorded at room temperature in the range of 200–1200 cm<sup>-1</sup> using Horiba Jobin-Yvon Lab Ram HR spectrometer with a 17 mW internal He–Ne (Helium–Neon) laser source of excitation wavelength of 632.8 nm. The catalyst samples in powder form (about 5–10 mg) were usually loosely spread onto a glass slide below the confocal microscope for measurements.

The acidity of the catalysts was measured by temperature programmed desorption of ammonia (TPD–NH<sub>3</sub>). In a typical experiment, 0.1 g of catalyst was loaded and pre-treated in He gas at 300 °C for 2 h. After pre-treatment the temperature was brought to 100 °C and the adsorption of NH<sub>3</sub> was carried out by passing a mixture of 10 % NH<sub>3</sub> balanced He gas over the catalyst for 1 h. The catalyst surface was flushed with He gas at the same temperature for 2 h to drive off physisorbed NH<sub>3</sub>. TPD of NH<sub>3</sub> was carried with a temperature ramp of 10 °C/min and the desorbed ammonia was monitored using thermal conductivity detector (TCD) of a gas chromatograph.

### 2.3 Catalytic Experiments

The reactions were performed in a 25 ml two neck round-bottom (RB) flask under reduced pressures. In a typical experiment, glycerol (2 g), urea (1.306 g) and catalyst (0.2 g) were taken in RB flask and heated in an oil bath in the temperature range of 100–160 °C with constant stirring. One neck of the RB flask was connected to vacuum line. Reaction was run under a reduced pressure in order to remove ammonia formed during the reaction. After completion of the reaction or stipulated time, methanol was added and the catalyst was separated by filtration. The

products were analyzed by a gas chromatograph (Shimadzu 2010) equipped with flame ionization detector using inno wax capillary column (diameter: 0.25 mm, length 30 m). Products were also identified by GC–MS (Shimadzu, GCMS-QP2010S) analysis.

### 3 Results and Discussion

#### 3.1 Catalyst Characterization

Table 1 shows the surface area of the catalysts along with surface density of  $\text{WO}_3$  on titania. From the Table 1 it was noticed that surface areas of the catalysts were increased from 41.6 to 62.6  $\text{m}^2/\text{g}$  with increase in  $\text{WO}_3$  loading from 5 to 15 %. Further increase in  $\text{WO}_3$  loading surface area of the catalyst was decreased. In the case of 25 %  $\text{WO}_3/\text{TiO}_2$  catalyst the surface area was 42  $\text{m}^2/\text{g}$ . The decrease in surface area of the catalysts beyond 15 wt% loading of  $\text{WO}_3$  was due to increase in the density of the tungsten oxide and partial plugging of the pores of titania. The tungsten oxide surface density values increased from 3.2 to 14.4  $\text{nm}^{-2}$  with increase in  $\text{WO}_3$  loading from 5 to 25 % on titania. The surface density of  $\text{WO}_3$  for monolayer coverage is about 5  $\text{nm}^2/\text{g}$  [39]. The surface density result suggests that the monolayer of  $\text{WO}_3$  was present for 10–15 %  $\text{WO}_3$  on  $\text{TiO}_2$  catalyst. However the surface density values were close to monolayer coverage for the catalysts with 15 %  $\text{WO}_3$  on  $\text{TiO}_2$ .

The crystalline structures of the  $\text{WO}_3/\text{TiO}_2$  catalysts were examined by XRD and patterns are shown in Fig. 1. The characteristic peaks located at  $2\theta$  of 25°, 37.6°, 47.9°, 53.7°, 54.9° and 62.5° were corresponds to the (101), (004), (200), (105), (211) and (204) crystal faces of anatase  $\text{TiO}_2$  [40]. However, characteristic peaks of rutile  $\text{TiO}_2$  were also observed at  $2\theta$  of 27.6°, 36.2°, 41.4°, 56.7° and 68.4° [41]. Intensities of the characteristic peaks related to anatase phase of titania were dominant than the rutile phase. This indicates that the anatase phase of titania is a major phase in all the catalysts. Furthermore, the crystalline  $\text{WO}_3$  phase was not detected for the catalysts with lower loadings of  $\text{WO}_3$  [42]. The presence of  $\text{WO}_3$  phase was observed for the catalysts with above 15 wt% of  $\text{WO}_3$  on  $\text{TiO}_2$ . The surface density values indicated the monolayer coverage of  $\text{WO}_3$  for 15 wt% of  $\text{WO}_3/\text{TiO}_2$  and the absence of crystalline phase of  $\text{WO}_3$

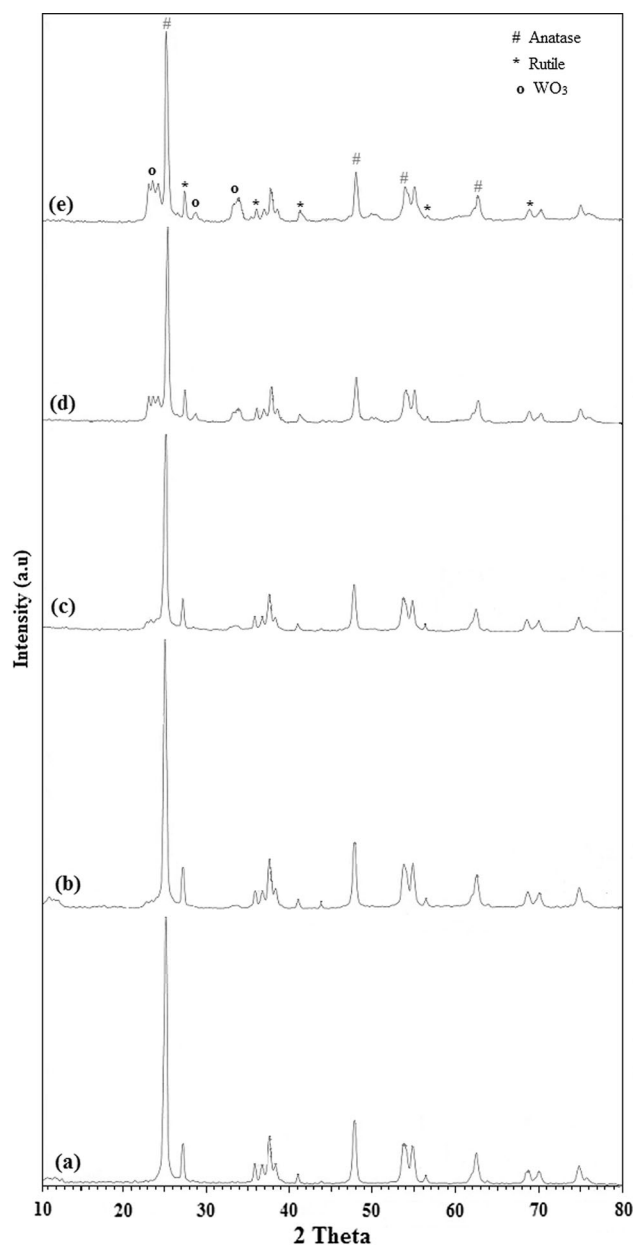


**Fig. 1** XRD patterns of  $\text{WO}_3/\text{TiO}_2$  catalysts. a 5 %  $\text{WO}_3/\text{TiO}_2$ , b 10 %  $\text{WO}_3/\text{TiO}_2$ , c 15 %  $\text{WO}_3/\text{TiO}_2$ , d 20 %  $\text{WO}_3/\text{TiO}_2$ , e 25 %  $\text{WO}_3/\text{TiO}_2$

indicates that tungsten nano crystalline particles might be formed. This indicates that the tungsten oxide species were highly dispersed on  $\text{TiO}_2$  at low loadings (<15 %) [43, 44].

**Table 1** Textural properties of  $\text{WO}_3/\text{TiO}_2$  catalysts

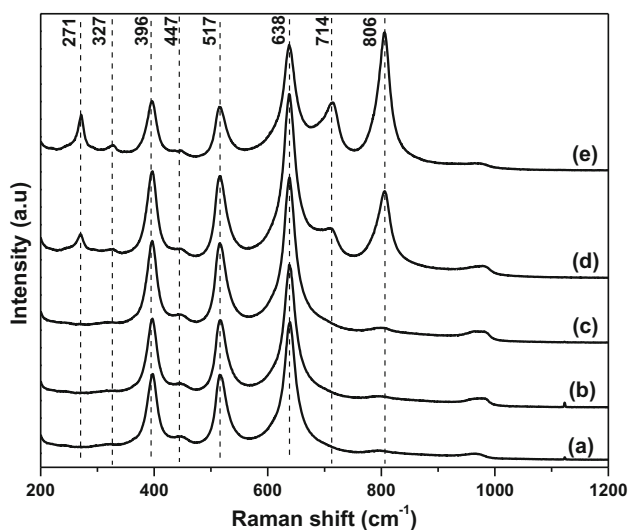
Catalyst	$S_{\text{BET}}$ ( $\text{m}^2\text{g}^{-1}$ )	Surface density of $\text{WO}_3$ ( $\text{nm}^{-2}$ )	Acidity (mmol/g)
5 % $\text{WO}_3/\text{TiO}_2$	41.6	3.2	0.417
10 % $\text{WO}_3/\text{TiO}_2$	50.6	5.2	0.452
15 % $\text{WO}_3/\text{TiO}_2$	62.6	6.2	0.554
20 % $\text{WO}_3/\text{TiO}_2$	51.1	10.1	0.473
25 % $\text{WO}_3/\text{TiO}_2$	44.8	14.4	0.404

Figure 2 shows the Laser Raman spectra of the catalysts. The Raman patterns were dominated by the bands related to titania. The predominant band at 396, 517 and 638  $\text{cm}^{-1}$  originates from the anatase phase of  $\text{TiO}_2$  [45, 46]. A broad and weak band at 447  $\text{cm}^{-1}$  was attributed to rutile phase of titania. A very weak Raman band related to  $\text{WO}_3$  was observed at 806  $\text{cm}^{-1}$  for the catalysts with below 15 % of  $\text{WO}_3$  on  $\text{TiO}_2$ . However, the intense bands at 271, 327, 714 and 806  $\text{cm}^{-1}$  related to crystalline  $\text{WO}_3$  observed for the catalysts with above 15 % of  $\text{WO}_3$  on titania [43]. From the laser Raman spectra it can be noted that  $\text{WO}_3$  was in highly dispersed state up to 15 %. XRD results were also in agreement with the results obtained by Laser Raman spectroscopy. The characterization results reveal that  $\text{WO}_3$  was well dispersed at lower loading and present in crystalline form at higher loadings.

Acidity of the catalysts was measured by TPD of ammonia. Acidity of the catalysts was measured based on desorbed ammonia and results are presented in Table 1. The acidity values of the catalysts indicate that, acidity was increased from 0.417 to 0.554 mmol/g with increase in  $\text{WO}_3$  loading from 5 to 15 %. Further increase in  $\text{WO}_3$  loading to 20 and 25 %, acidity of the catalysts was decreased to 0.473 and 0.404 mmol/g, respectively. The decrease in acidity value was due to aggregation of  $\text{WO}_3$  species on titania at higher loading, which was confirmed by XRD. From these results it can be concluded that 15 %  $\text{WO}_3/\text{TiO}_2$  catalyst possess more number of acidic sites.

### 3.2 Influence of $\text{WO}_3$ Loading on Titania for Carbonylation of Glycerol

Effect of the  $\text{WO}_3$  loading on  $\text{TiO}_2$  on carbonylation of glycerol was studied and results are shown in Fig. 3.



**Fig. 2** Laser Raman spectra of  $\text{WO}_3/\text{TiO}_2$  catalysts. *a* 5 %  $\text{WO}_3/\text{TiO}_2$ , *b* 10 %  $\text{WO}_3/\text{TiO}_2$ , *c* 15 %  $\text{WO}_3/\text{TiO}_2$ , *d* 20 %  $\text{WO}_3/\text{TiO}_2$ , *e* 25 %  $\text{WO}_3/\text{TiO}_2$

Carbonylation of glycerol over titania and tungsten oxide were also studied in order to compare the efficiency of the  $\text{WO}_3/\text{TiO}_2$  catalysts. About 19.3 % of conversion with glycerol carbonate selectivity of 10.5 % was observed in the absence of catalyst. Glycerol conversion was increased in the case of titania and tungsten oxides. The observed glycerol conversions were 26.8 and 32.3 % for  $\text{WO}_3$  and  $\text{TiO}_2$ , respectively. In the case of  $\text{WO}_3/\text{TiO}_2$  catalysts, the conversion of glycerol increased from 38.2 to 73 % with increase in  $\text{WO}_3$  content from 5 to 15 %. Further increase in  $\text{WO}_3$  loading on titania, a decrease in conversion of glycerol was observed. Glycerol conversion was only 33.3 % in the case of 25 %  $\text{WO}_3/\text{TiO}_2$  catalyst. The activity exhibited by catalysts can be correlated to the catalysts characteristics. XRD and Raman patterns showed that, at lower  $\text{WO}_3$  loading (15 %) the  $\text{WO}_3$  species were well dispersed on the titania support without significant crystallization. The high catalytic activity of 15 %  $\text{WO}_3/\text{TiO}_2$  catalyst was due to high dispersion of  $\text{WO}_3$  on titania which results in high surface area and acidity (Table 1). However, beyond 15 % loading crystalline phase of  $\text{WO}_3$  formed due to the aggregation of tungsten oxide species on titania. Therefore, the promoting effect of  $\text{WO}_3$  loading (15 wt%) was mainly attributed to the number of surface active  $\text{WO}_3$  sites. In contrast, as discussed above the crystalline  $\text{WO}_3$  appeared at higher loadings (>15 %) responsible for decrease in catalytic activity.

### 3.3 Effect of Catalyst Calcination Temperature on Glycerol Conversion

In order to know the surface, structural changes in the catalyst with increase in calcination temperature and its

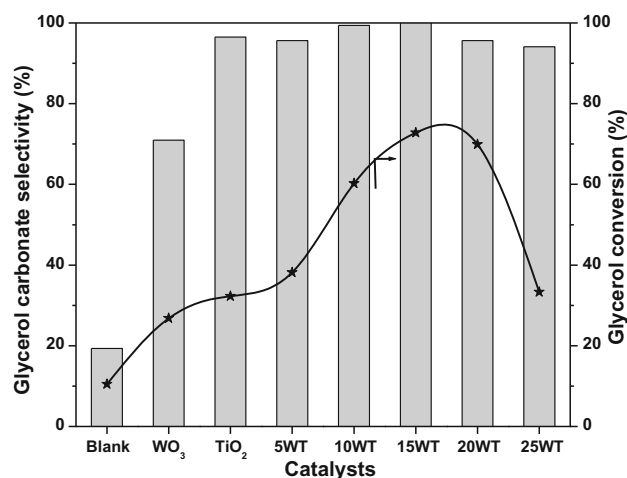


**Fig. 3** Influence of  $\text{WO}_3$  loading on  $\text{TiO}_2$  on carbonylation of glycerol with urea. Reaction conditions: glycerol (2 g), urea (1.306 g), catalyst weight (0.2 g), reaction temperature (140 °C)

influence on glycerol conversion, the most active catalyst 15 %  $\text{WO}_3/\text{TiO}_2$  was subjected to calcination at different temperatures in the range of 400–700 °C. Catalytic activity of these catalysts was tested for carbonylation of glycerol and results are shown in Fig. 4. From the activity results it was observed that with increase in calcination temperature from 400 to 500 °C, conversion of glycerol drastically increased from 23.3 to 73 % and there was no change in selectivity towards glycerol carbonate. Further increase in calcination temperature to 600 and 700 °C, conversion of the glycerol was decreased to 68.8 and 19.5 %, respectively and there was no change in selectivity. Compared to other catalysts, catalyst calcined at 500 °C exhibited high activity in glycerol carbonate synthesis.

In order to elucidate the variation in catalytic activity and structural changes in 15 %  $\text{WO}_3/\text{TiO}_2$  catalyst with calcination temperature, these catalysts were characterized by XRD, laser Raman and TPD of  $\text{NH}_3$ .

### 3.4 Characterization of 15 % $\text{WO}_3/\text{TiO}_2$ Catalyst Calcined at Different Temperatures

The 15 %  $\text{WO}_3/\text{TiO}_2$  catalyst calcined at various temperatures in the range of 400–700 °C were characterized by XRD and the results are shown in Fig. 5. All the catalysts exhibited characteristic peaks of titania as discussed earlier in the Sect. 3.1. From the figure it can be noticed that catalyst calcined at 400 and 500 °C, no patterns related to crystalline  $\text{WO}_3$  were observed. This indicates that  $\text{WO}_3$  was highly dispersed on titania in both the catalysts. Increase in calcination temperature to 600 °C, crystallinity of the  $\text{WO}_3$  was started and patterns related to tungsten oxide were clearly seen in the case of catalyst calcined at 700 °C [47]. Intensities of the characteristic peaks related

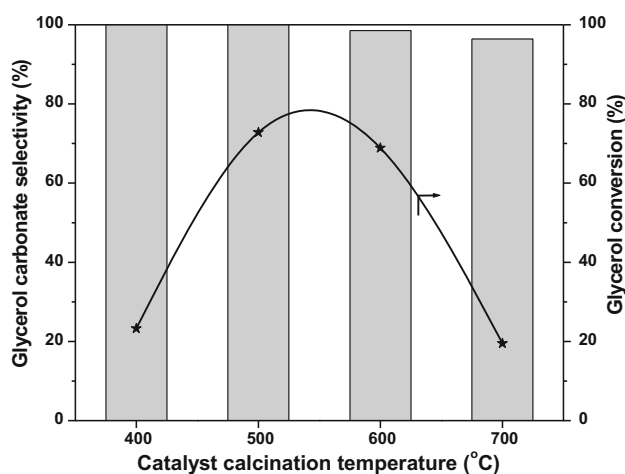


**Fig. 4** Effect of 15 %  $\text{WO}_3/\text{TiO}_2$  catalyst calcination temperature on glycerol carbonate yield. Reaction conditions: glycerol (2 g), urea (1.306 g), catalyst weight (0.2 g), reaction temperature (140 °C)

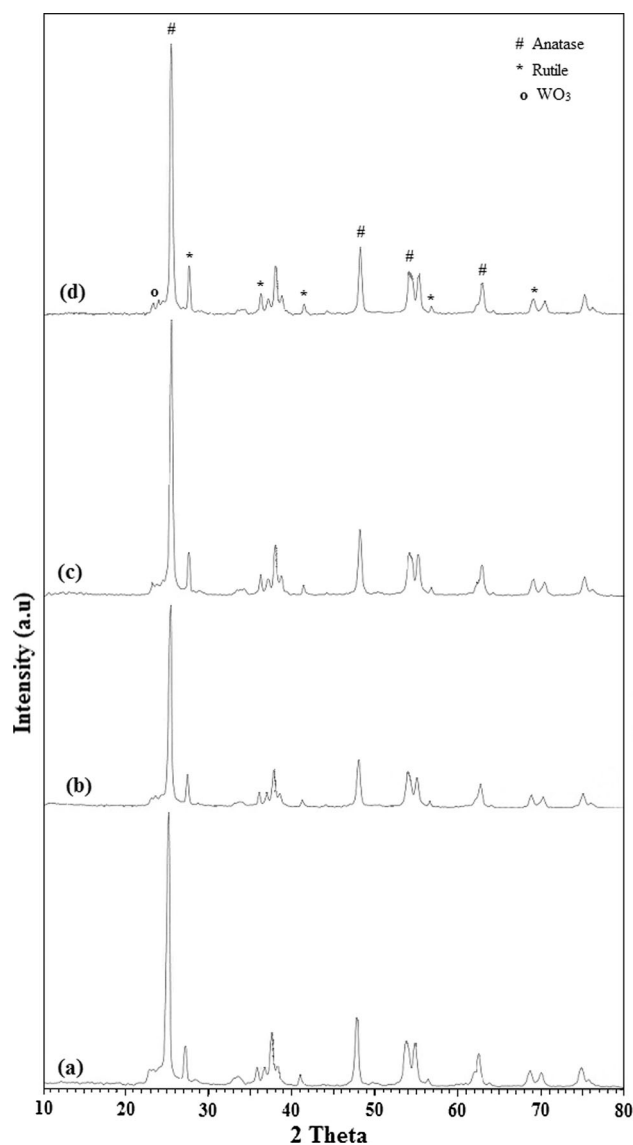


**Fig. 5** XRD profiles of 15 %  $\text{WO}_3/\text{TiO}_2$  catalyst calcined at different temperatures a 400 °C, b 500 °C, c 600 °C, and d 700 °C

to anatase phase of titania were also increased with increase in calcination temperature. These results indicate that  $\text{WO}_3$  was highly dispersed state at calcination temperatures below 600 °C.

Figure 6 shows the Laser Raman spectra of 15 %  $\text{WO}_3/\text{TiO}_2$  catalyst calcined in the range of 400–700 °C. No bands related to crystalline  $\text{WO}_3$  were observed for the catalysts calcined in the range of 400–600 °C. However, in the case of catalyst treated at 600 °C, intensity of the weak band at 806  $\text{cm}^{-1}$  was slightly increased. This indicates that aggregation of  $\text{WO}_3$  species started at 600 °C. Whereas, catalyst treated at 700 °C showed intense bands at 271, 714 and 806  $\text{cm}^{-1}$  related to crystalline tungsten oxide [48, 49] which were assigned to the symmetric stretching mode of W–O, bending mode of W–O and the

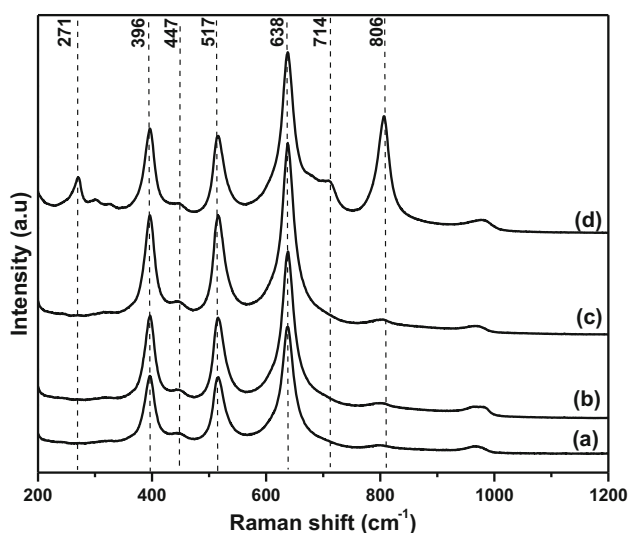


**Fig. 6** Raman spectra of 15 %  $\text{WO}_3/\text{TiO}_2$  catalyst calcined at different temperatures *a* 400 °C, *b* 500 °C, *c* 600 °C, *d* 700 °C

deformation mode of W–O–W, respectively [50]. From the XRD and Laser Raman results it can be concluded that  $\text{WO}_3$  was highly dispersed state when calcined at lower temperatures and  $\text{WO}_3$  aggregates formed above 600 °C.

The decrease in catalytic activity with increase in catalyst calcination temperature can be correlated to the characterization results obtained from XRD and laser Raman studies. Tungsten oxide was highly dispersed in the case of lower calcination temperatures (400–500 °C). At high calcination temperatures crystalline form of  $\text{WO}_3$  was observed. From the TPD of ammonia results it was observed that total acidity was more for 15 %  $\text{WO}_3/\text{TiO}_2$  catalyst calcined at 500 °C. This catalyst possess high surface area and total acidity compared to other catalysts and there by exhibited high activity towards carbonylation of glycerol.

### 3.5 Influence of Support

In order to know the influence of support, the most active 15 %  $\text{WO}_3/\text{TiO}_2$  catalyst was compared with  $\text{WO}_3$  supported on different supports like  $\text{Nb}_2\text{O}_5$ ,  $\text{SiO}_2$ ,  $\text{ZrO}_2$ ,  $\text{MoO}_3$ ,  $\text{Al}_2\text{O}_3$  and results are shown in Table 2. The content of  $\text{WO}_3$  was kept constant as 15 wt% on all these supports. From the activity results it was observed that 15 %  $\text{WO}_3/\text{Al}_2\text{O}_3$  exhibited low carbonylation activity compared to all other supported catalysts. Conversion of the glycerol was only 19.5 % with 77.1 % selectivity towards glycerol carbonate was observed for alumina supported catalysts. In the case of 15 %  $\text{WO}_3/\text{ZrO}_2$  and 15 %  $\text{WO}_3/\text{Nb}_2\text{O}_5$  catalysts, conversion of glycerol was about 30 % and selectivity towards glycerol carbonate was 97.1 %. When  $\text{WO}_3$  supported on silica, con-

**Table 2** Comparison of catalytic activity of  $\text{WO}_3$  supported on different supports

S.no	Support	Glycerol conversion	GC selectivity
1	$\text{ZrO}_2$	29.94	97.09
2	$\text{Nb}_2\text{O}_5$	30.18	97.12
3	$\text{SiO}_2$	46.63	95.45
4	$\text{TiO}_2$	72.78	100
5	$\text{MoO}_3$	37.54	99.59
6	$\text{Al}_2\text{O}_3$	19.5	77.05

Reaction conditions: glycerol (2 g), urea (1.306 g), catalyst weight (0.2 g), reaction temperature (140 °C), reaction time (4 h)

version of the glycerol increased to 46.6 % and selectivity slightly decreased to 95.5 %. Selectivity towards glycerol carbonate was near 100 % in the case of  $\text{WO}_3$  supported on  $\text{TiO}_2$  and  $\text{MoO}_3$  supports. However, maximum conversion of 73 % was achieved in the case of 15 %  $\text{WO}_3/\text{TiO}_2$  and conversion of glycerol was only 37.5 % for 15 %  $\text{WO}_3/\text{MoO}_3$  catalyst. The 15 %  $\text{WO}_3/\text{TiO}_2$  catalyst showed higher activity compared to all other catalysts. The activities of the catalysts were in the order of 15 %  $\text{WO}_3/\text{TiO}_2 > 15$  %  $\text{WO}_3/\text{SiO}_2 > 15$  %  $\text{WO}_3/\text{MoO}_3 > 15$  %  $\text{WO}_3/\text{Nb}_2\text{O}_5 > 15$  %  $\text{WO}_3/\text{ZrO}_2 > 15$  %  $\text{WO}_3/\text{Al}_2\text{O}_3$ .

### 3.6 Optimization of Reaction Parameters

In order to optimize the various reaction parameters such as effect of reaction temperature, effect of glycerol to urea molar ratio, and effect of catalyst weight, the most active catalyst 15 %  $\text{WO}_3/\text{TiO}_2$  calcined at 500 °C was used.

#### 3.6.1 Effect of Reaction Temperature

Reaction temperature has a significant effect on the overall conversion of glycerol and selectivity to glycerol carbonate during glycerolysis of urea. Hence, the effect of reaction temperature was studied over 15 wt%  $\text{WO}_3/\text{TiO}_2$  catalyst and the results are presented in Fig. 7. Conversion of glycerol was only 3.1 % when reaction was carried at 100 °C and increased with increase in reaction temperature. When the temperature increased from 100 to 140 °C glycerol conversion was increased from 3.1 to 73 %. The selectivity towards glycerol carbonate was almost constant (about 100 %). Further increase in reaction temperature to 160 °C, there is no considerable increase in glycerol conversion. However, selectivity towards glycerol carbonate was decreased to 77.4 %. This might be due to decomposition/decarbonylation of the glycerol carbonate at higher temperatures. For high conversion of glycerol and glycerol carbonate selectivity the optimum temperature is 140 °C.

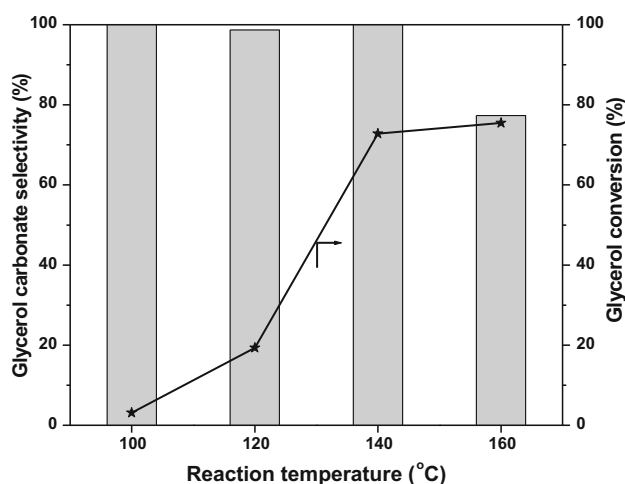


**Fig. 7** Effect of reaction temperature on glycerol carbonylation activity. Reaction conditions: glycerol (2 g), urea (1.306 g), catalyst weight (0.2 g), reaction time (4 h)

### 3.6.2 Effect of Glycerol to Urea Molar Ratio

The influence of glycerol to urea molar ratio on the formation of glycerol carbonate was studied and the results are presented in Fig. 8. In the case of glycerol to urea molar ratio of 1:0.5, conversion of glycerol was only 28 %. Varying in glycerol to the urea molar ratio from 1:0.5 to 1:3 conversion of glycerol increased from 28 to 79.8 %. In other words, with increase in urea concentration (or decrease in glycerol concentration) conversion of glycerol was increased. However, selectivity towards glycerol carbonate was decreased from 100 to 90.3 % with increase in urea concentration. This might be due to reaction of glycerol carbonate with available urea molecule to yield

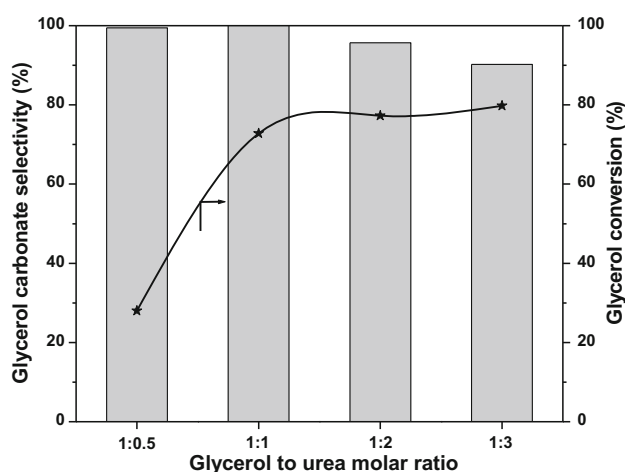


**Fig. 8** Influences of glycerol to urea molar ratio on carbonylation activity. Reaction conditions: catalyst weight (0.2 g), reaction temperature (140 °C), reaction time (4 h)

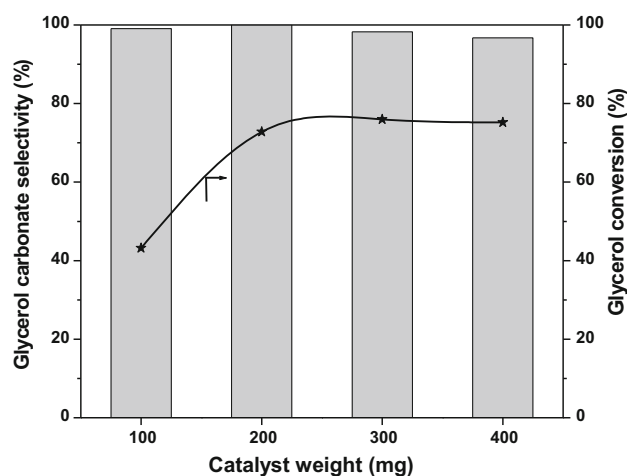


**Fig. 9** Effect of catalyst weight on glycerol conversion and glycerol carbonate selectivity. Reaction conditions: glycerol (2 g), urea (1.306 g), reaction temperature (140 °C), reaction time (4 h)

side products such as, (2-oxo-1,3-dioxolan-4-yl) methyl-carbamate [25]. From the Fig. 8, it was concluded that glycerol to urea molar ratio 1:1 is optimum for high glycerol conversion and glycerol carbonate selectivity.

### 3.6.3 Effect of Catalyst Weight

The effect of catalyst amount on conversion of glycerol was studied and the results are shown in Fig. 9. As the concentration of catalyst increased more active sites were available for glycerolysis of urea. From the figure it was observed that the conversion of glycerol increased from 43.2 to 76 % with increase in catalyst weight from 100 to 300 mg. Further increase in catalyst weight to 400 mg, glycerol conversion was almost constant. When the catalyst concentration was 200 mg, selectivity towards glycerol carbonate was about 100 %. Further increase in catalyst concentration to 300–400 mg glycerol carbonate selectivity was marginally decreased. These results suggest that 200 mg of the catalyst was optimum for high conversion of glycerol and selectivity towards glycerol carbonate.

### 3.7 Reusability of the Catalyst

Recycling experiments were carried out to investigate the stability and reusability of the 15 %  $\text{WO}_3/\text{TiO}_2$  catalyst. In each cycle, the used catalyst was separated by filtration and washed with methanol to remove the products adhering to the surface of catalyst, dried in oven at 100 °C. Then this was reused directly for the next run without any pretreatment. Figure 10 shows the recycling results of the catalyst. Conversion of glycerol and selectivity towards glycerol carbonate decreased slightly with number of catalyst

recycles. Fresh catalyst exhibited 73 % conversion with 100 % glycerol carbonate selectivity. After the third recycle, conversion of glycerol was decreased to 66.2 %. Compared to the fresh catalyst about 6.6 % decrease in glycerol conversion was observed for reused one (3rd recycle) and there was no appreciable decrease in glycerol carbonate selectivity. The loss in activity is attributed to physical loss of catalyst during reuse. The observed glycerol carbonate selectivity after third recycle was 96 %. These results indicated that catalyst was active upon reuse.

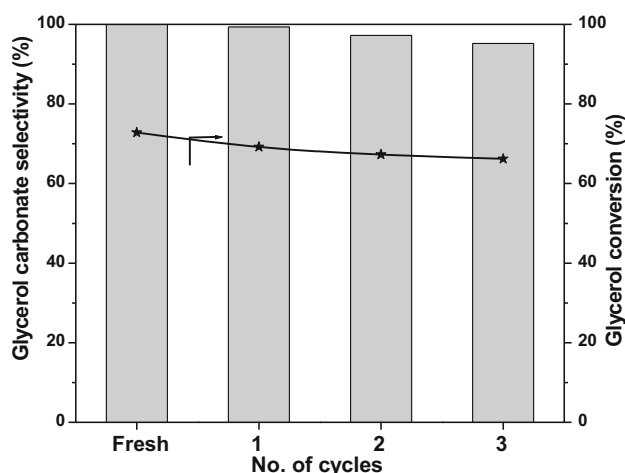


**Fig. 10** Reusability study of 15 %  $\text{WO}_3/\text{TiO}_2$  catalyst for carbonylation of glycerol with urea. Reaction conditions: glycerol (2 g), urea (1.306 g), catalyst weight (0.2 g), reaction temperature (140 °C), reaction time (4 h)

### 3.8 Comparison of the Catalytic Activity of the 15 % $\text{WO}_3/\text{TiO}_2$ with the Reported Catalysts

Table 3 shows the comparison of catalytic activity of 15 %  $\text{WO}_3/\text{TiO}_2$  catalyst with other reported catalysts. The previously reported metal exchanged heteropoly acid catalysts such as  $\text{Zn}_1\text{TPA}$ ,  $\text{Sm}_{0.66}\text{TPA}$  exhibited low glycerol conversion and glycerol carbonate yields [30, 31]. Where as in the case of silicotungstic acid supported on MCM-41, conversion of glycerol was 75 % and glycerol carbonate yield was only 57.8 % after 8 h of reaction time and at high temperature (150 °C) [34]. Zinc monoglycerolate [33] and Sn- $\beta$  zeolite [13] catalysts exhibited high glycerol conversion at longer reaction times (>5 h). Glycerol carbonate yields are low in the case of supported gold catalysts even at high reaction temperatures (150 °C) [27]. Zn-Y zeolite [35], BA900 [36], gypsum [37], ionic liquid [38] etc. catalysts exhibited greater than 92 % glycerol conversion and >83 % glycerol carbonate yields only at 150 °C. However, the glycerol carbonate yield was highest (92.7 %) only in the case of Zn-Y zeolite [35]. Zirconium phosphate catalyst showed 76 % glycerol carbonate yield at 140 °C and 3 h of reaction time [29]. However the glycerol conversion was low compared to other catalysts [33, 35–38]. The previously reported mixed oxide catalyst (SW21) exhibited only 49.7 % glycerol carbonate yield with 52.1 % glycerol conversion [32]. The present 15 %  $\text{WO}_3/\text{TiO}_2$  catalyst exhibited 100 % glycerol conversion at relatively lower reaction temperature of 140 °C. The glycerol carbonate yield (73 %) also comparable to other reported catalysts. In conclusion, the present catalyst is reusable and exhibited

**Table 3** Comparison of catalytic activity of the 15 %  $\text{WO}_3/\text{TiO}_2$  catalyst with other reported catalysts

Catalyst	Reaction temperature (°C)	Reaction time (h)	Glycerol conversion (%)	Glycerol carbonate yield (%)	Reference
15 % $\text{WO}_3/\text{TiO}_2$	140	4	100	73.0	Present work
$\text{Zn}_1\text{TPA}$	140	4	69.2	68.8	[31]
$\text{Sm}_{0.66}\text{TPA}$	140	4	49.5	42.3	[30]
SW21	140	4	52.1	49.7	[32]
Zr-P	140	3	80	76	[29]
Zinc monoglycerolate	140	7	98	83.3	[33]
Sn- $\beta$ zeolite	145	5	70	26	[13]
$\text{Au}/\text{Fe}_2\text{O}_3$	150	4	80	39	[27]
2.5 % $\text{Au}/\text{Nb}_2\text{O}_5$	150	4	66	21	[27]
30 % $\text{SiW}_{12}/\text{MCM-41}$	150	8	75	57.8	[34]
Zn-Y zeolite	150	3	94.6	92.7	[35]
BA900	150	4	93.6	84.4	[36]
Gypsum ( $\beta$ -phase)	150	4	92.8	83.6	[37]
$(\text{HEIm})_2\text{ZnCl}_2$	150	4	92.8	86.6	[38]



complete conversion of glycerol compared to other solid acid catalysts.

## 4 Conclusions

Tungsten oxide supported on titania catalysts were prepared for the synthesis of glycerol carbonate from glycerol and urea. The interaction between tungsten oxide and titania influences the activity of the catalysts. The content of  $\text{WO}_3$  on support and calcination temperature influences the activity of the catalyst. Highly dispersed amorphous  $\text{WO}_3$  species are more active for the synthesis of glycerol carbonate from glycerol and urea. The catalyst with 15 wt%  $\text{WO}_3$  on  $\text{TiO}_2$  calcined at 500 °C showed highest activity towards the synthesis of glycerol carbonate.  $\text{TiO}_2$  is the best support for  $\text{WO}_3$  compared to other supports. Various reaction parameters were optimized and the catalyst is reusable with consistent activity without any pretreatment.

**Acknowledgments** The authors thank to Council of Scientific Industrial Research (CSIR), India for the financial support in the form of Indus magic (CSC-0123) Project under 12th Five Year Program.

## References

- Zheng Y, Chen X, Shen Y (2008) *Chem Rev* 108:5253–5277
- Balaraju M, Rekha V, Sai Prasad PS, Devi BLAP, Prasad RBN, Lingaiah N (2009) *Appl Catal A* 354:82–87
- Pachauri N, He B (2006) ASABE annual international meeting, Portland, Oregon 9–12 July
- Pagliaro M, Ciriminna R, Kimura H, Rossi M, Pina CD (2007) *Angew Chem Int Ed* 46:4434–4440
- Pathak K, Reddy KM, Bakhshi NN, Dalai AK (2010) *Appl Catal A* 372:224–238
- Balaraju M, Rekha V, Devi BLAP, Prasad RBN, Prasad PSS, Lingaiah N (2010) *Appl Catal A* 384:107–114
- Behr A, Eilting J, Irawadi K, Leschinski J, Lindner F (2008) *Green Chem* 10:13–30
- Rokicki G, Rakoczy P, Parzuchowski P, Sobiecki M (2005) *Green Chem* 7:529–539
- Mei HJ, Zhong ZL, Long FF, Zhuo RX (2006) *Macromol Rapid Commun* 27:1894–1899
- Ubaghs L, Fricke N, Keul H, Hocker H (2004) *Macromol Rapid Commun* 25:517–521
- Simao AC, Pukleviciene BL, Rousseau C, Tatibouet A, Cassel S, Sackus A, Rauter AP, Rollin P (2006) *Lett Org Chem* 3:744–748
- Shaikh AG, Sivaram S (1996) *Chem Rev* 96:951–976
- Climent MJ, Corma A, Frutos P, Iborra S, Noy M, Velty A, Concepcion P (2010) *J Catal* 269:140–149
- Parka J-H, Choia JS, Wooa SK, Leea SD, Cheong M, Kimb HS, Leea H (2012) *Appl Catal A* 433–434:35–40
- Casiello M, Monopoli A, Cotugno P, Milella A, Dell'Anna MM, Ciminale F, Nacci A (2014) *J Mol Catal A* 381:99–106
- Lee KH, Park CH, Lee EY (2010) *Bioprocess Biosyst Eng* 33:1059–1065
- Kim SC, Kim YH, Lee H, Yoon DY, Song BK (2007) *J Mol Catal B* 49:75–78
- Pyo SH, Persson P, Lundmark S, Kaul RH (2011) *Green Chem* 13:976–982
- Seong PJ, Jeon BW, Lee M, Cho DH, Kim DK, Jung KS, Kim SW, Han SO, Kim YH, Park C (2011) *Enzyme Microb Technol* 48:505–509
- Li JB, Wang T (2011) *J Chem Thermodyn* 43:731–736
- Vieville C, Yoo JW, Pelet S, Mouloungui Z (1998) *Catal Lett* 56:245–247
- Sasa T, Okutsu M, Uno M (2009) *JP Patent* 2007-234982 2009067689
- Yoo JW, Mouloungui Z (2003) *Stud Surf Sci Catal* 146:757–760
- Okutsu M, Kitsuki T (2000) *WO Patent* 2000-JP1072 2000050415
- Okutsu M (2007) *JP Patent* 2005-222721 2010040768
- Wang L, Ma Y, Wang Y, Liu S, Deng Y (2011) *Catal Commun* 12:1458–1462
- Hammond C, Sanchez JAL, Ab Rahim MH, Dimitratos N, Jenkins RL, Carley AF, He Q, Kiely CJ, Knight DW, Hutchings GJ (2011) *Dalton Trans* 40:3927–3937
- Marcos FR, Casilda VC, Banares MA, Fernandez JF (2010) *J Catal* 275:288–296
- Areata M, Dibenedetto A, Nocito F, Ferragina C (2009) *J Catal* 268:106–114
- Ramesh Kumar Ch, Jagadeeswaraiah K, Sai Prasad PS, Lingaiah N (2012) *ChemCatChem* 4:1360–1367
- Jagadeeswaraiah K, Ramesh Kumar Ch, Sai Prasad PS, Lingaiah N (2014) *Catal Sci Technol* 4:2969–2977
- Jagadeeswaraiah K, Ramesh Kumar Ch, Sai Prasad PS, Lorient S, Lingaiah N (2014) *Appl Catal A* 469:165–172
- Turney TW, Patti A, Gates W, Shaheen U, Kulasegaram S (2013) *Green Chem* 15:1925–1931
- Narkhede N, Patel A (2015) *RSC Adv* 5:52801–52808
- Marakatti VS, Halgeri AB (2015) *RSC Adv* 5:14286–14293
- Indran VP, Zuhaimi NAS, Deraman MA, Maniam GP, Yusoff MM, Hin TYY, Rahim MHA (2014) *RSC Adv* 4:25257–25267
- Zuhaimi NAS, Indran VP, Deraman MA, Mudrikah NF, Maniam GP, Yap YHT, Rahim MHA (2015) *Appl Catal A* 502:312–319
- Kim DW, Park DW (2014) *J Nanosci Nanotechnol* 14:4632–4638
- Soung Kim D, Ostromecki M, Wachs IE (1996) *J Mol Catal A* 106:93–102
- Ramesh Kumar Ch, Sai Prasad PS, Lingaiah N (2011) *J Mol Catal A* 350:83–90
- Jiang YH, Sun YM, Zhao CX, Wu M, Yin HB, Chen KM (2007) *New Chem Mater* 35:28–30
- Yang H, Shi R, Zhang K, Hu Y, Tang A, Li X (2005) *J Alloy Compd* 398:200–202
- Akurati KK, Vital A, Dellemann JP, Michalow K, Graule T, Ferri D, Baiker A (2008) *Appl Catal B* 79:53–62
- Kobayashi M, Miyoshi K (2007) *Appl Catal B* 72:253–261
- Martin C, Solana G, Rives V, Marci G, Palmisano L, Sclafani A (1997) *Catal Lett* 49:235–243
- Chen X, Mao SS (2007) *Chem Rev* 107:2891–2959
- Liu G, Wang X, Wang X, Han H, Li C (2012) *J Catal* 293:61–66
- Jin R, Xia X, Dai W, Deng JF, Li H (1999) *Catal Lett* 62:201–207
- Pae Y, Bae MH, Park WC, Sohn JR (2004) *Bull Korean Chem Soc* 25:1881–1888
- Vuurman MA, Wachs IE (1991) *J Phys Chem* 95:9928–9937